Published in final edited form as:
Curr Biol. 2012 March 20; 22(6): 545–552. doi:10.1016/j.cub.2012.02.005.

Spatial Parkin Translocation and Degradation of Damaged Mitochondria Via Mitophagy in Live Cortical Neurons

Qian Cai[1,2,#], **Hesham Mostafa Zakaria**[1,3], **Anthony Simone**[1], and **Zu-Hang Sheng**[1,#]

[1]Synaptic Functions Section, The Porter Neuroscience Research Center, National Institute of Neurological Disorders and Stroke, National Institutes of Health, Room 2B-215, 35 Convent Drive, Bethesda, Maryland 20892-3706, USA

[2]Department of Cell Biology and Neuroscience, Rutgers, The State University of New Jersey, 604 Allison Road, Piscataway, NJ 08854-6999, USA

[3]Howard Hughes Medical Institute-National Institutes of Health Research Scholars Program

Summary

Mitochondria are essential for neuronal survival and function. Proper degradation of aged and damaged mitochondria through mitophagy is a key cellular pathway for mitochondrial quality control. Recent studies have indicated that PINK1/Parkin-mediated pathways ensure mitochondrial integrity and function [1–8]. Translocation of Parkin to damaged mitochondria induces mitophagy in many non-neuronal cell types [9–16]. However, evidence showing Parkin translocation in primary neurons is controversial [9,15,17,18], leaving unanswered questions as to how and where Parkin-mediated mitophagy occurs in neurons. Here, we report the unique process of dissipating mitochondrial $\Delta\psi_m$-induced and Parkin-mediated mitophagy in mature cortical neurons. Compared with non-neuronal cells, neuronal mitophagy is a much slower and compartmentally restricted process, coupled with reduced anterograde mitochondrial transport. Parkin-targeted mitochondria are accumulated in the somatodendritic regions where mature lysosomes are predominantly located. Time-lapse imaging shows dynamic formation and elimination of Parkin- and LC3-ring like structures surrounding depolarized mitochondria through the autophagy-lysosomal pathway in the soma. Knocking down Parkin in neurons impairs the elimination of dysfunctional mitochondria. Thus, our study provides neuronal evidence for dynamic and spatial Parkin-mediated mitophagy, which will help us understand whether altered mitophagy contributes to pathogenesis of several major neurodegenerative diseases characterized by mitochondrial dysfunction and impaired transport.

[#]Correspondence should be addressed to Z.-H. Sheng (shengz@ninds.nih.gov) or Q. Cai (Cai@Biology.Rutgers.Edu).

COMPETING INTERESTS STATMENT

The authors declare no competing financial interests.

Animal care and use were carried out in accordance with NIH guidelines and approved by the NIH, NINDS/NIDCD Animal Care and Use Committee.

Supplemental information

Supplemental information including four Supplemental Figures, two Movies, and Experimental Procedures and Supplemental References can be found with this article online.

Keywords

mitochondria; Parkin; lysosome; autophagosome; autophagy; depolarization; mitochondrial mobility; neuronal mitophagy; mitochondrial quality control

Results and Discussion

Mitochondrial Depolarization Induces Slower Parkin Translocation in Mature Neurons

To examine whether mitochondrial depolarization induces Parkin translocation in neurons, we performed three lines of experiments. First, we treated mouse cortical neurons expressing YFP-Parkin and DsRed-Mito at 9–10 days *in vitro* (DIV) for 24 hr with vehicle DMSO as a control, 10μM CCCP (a $\Delta\psi_m$ dissipating reagent), or 10μM CCCP with lysosomal inhibitors (LIs: 10μM Pepstatin A and 10μM E64D). While YFP-Parkin was diffuse in the cytosol of DMSO-treated control neurons (n=435), it redistributed to mitochondria in 26.67±4.46% of neurons (n=420) treated with CCCP and in 55.87±6.57% of neurons treated with CCCP/LIs (n=570) (Figures 1A and 1B). Treatment with CCCP/LIs doubled the percentage of neurons with Parkin translocation relative to CCCP alone ($p<0.001$), suggesting that lysosomal degradation capacity has a significant impact on the clearance of Parkin-targeted mitochondria via mitophagy in neurons. Second, we co-immunostained similarly treated neurons with antibodies against neuronal marker MAP2 and mitochondrial markers TOM20 (an outer membrane protein) or cytochrome *c* (a dynamic inter-membrane space protein). YFP-Parkin was recruited to mitochondria labeled with TOM20 or cytochrome *c* (Figure 1C) in CCCP-treated neurons, but not in DMSO controls. To examine Parkin translocation kinetics, we imaged neurons at various time points during CCCP treatment. Parkin translocation between 0.5–6 hr was exceptionally rare. Parkin-ring like structures surrounding fragmented mitochondria were occasionally observed at as early as 12 hr and became increasingly frequent after 18 hr of CCCP treatment (Figure 1D).

To determine whether endogenous Parkin undergoes similar translocation after depolarization, we immunostained cortical neurons at DIV10 with an anti-Parkin antibody following 24-hr CCCP/LIs treatment. While endogenous Parkin appears as a diffuse pattern or as small puncta not co-localized with mitochondria in DMSO-treated neurons, CCCP/LIs induces endogenous Parkin recruitment to mitochondria (Figure 1E). Alternatively, we isolated the mitochondria-enriched membrane fraction from cultured cortical neurons at DIV13 following the same treatment. While the majority of Parkin was in the cytosolic fraction, treatment with CCCP/LIs induced endogenous Parkin to associate with the mitochondria-enriched membrane (Figure 1F). Quantitative analysis showed a 2-fold (2.28±0.31) increase in Parkin intensity in the mitochondrial fractions following treatment with CCCP/LIs compared with DMSO ($p=0.0014$, n=3). We also observed elevated levels of the autophagic markers LC3-II and p62/SQSTM1 associated with the mitochondria-enriched membrane fraction. Altogether, these results indicate that mitochondrial depolarization can induce the recruitment of both exogenous and endogenous Parkin in mature neurons.

A gradual but slow increase in Parkin translocation during prolonged CCCP treatment argues against the possibility that CCCP becomes less effective over time in medium. Spiked CCCP media, which had been incubated with neurons for 24 hr, was still effective and sufficient to induce 23.95±2.49% of cultured neurons (fresh) to display Parkin translocation, a percentage close to that when using fresh CCCP (26.67±4.46%) at the same concentration (Figure S1). These results suggest that Parkin-mediated mitophagy in neurons is a much slower process than in other cell types reported. Treating HeLa cells with 10μM

CCCP or SH-SY5Y cells with 20μM CCCP can induce Parkin association with mitochondria in ~80% of cells within 1–2 hr [9–11, 17].

Parkin Is Selectively Recruited to Depolarized Mitochondria

To examine whether Parkin-targeted mitochondria display dissipated $\Delta\psi_m$, we pulsed live neurons expressing YFP-Parkin and CFP-Mito with tetramethylrhodamine ethyl ester (TMRE), a $\Delta\psi_m$-dependent dye. Active/healthy mitochondria will accumulate TMRE to have higher TMRE intensity. In DMSO-treated neurons or neurons recovered from CCCP treatment (no Parkin translocation), the majority of CFP-Mito-labeled mitochondria were co-labeled by TMRE, reflecting their electrochemically active status (Figure 2A). In contrast, somatic mitochondria with YFP-Parkin translocation displayed reduced or no TMRE staining, suggesting that YFP-Parkin is selectively recruited to depolarized mitochondria (Figures 2A and 2B). We quantified the TMRE mean intensity in somas and normalized to that in DMSO control neurons (Figure 2C). Neurons with Parkin translocation exhibited a 48.3±4.7% (n=17; $p<0.001$) reduction in the TMRE mean intensity relative to recovered neurons (95.9±5.3% n=16) and DMSO-treated controls (n=16). Time-lapse TMRE imaging in live cortical neurons demonstrates that acute incubation with 10μM CCCP during an 11-min recording is sufficient to globally depolarize $\Delta\psi_m$ (Figure S2B). Furthermore, Parkin was gradually recruited to mitochondria in the soma during a 52-min recording time (Figure 2D, Movie 1).

To determine whether endogenous Parkin is critical for eliminating mitochondria with dissipated $\Delta\psi_m$, we suppressed Parkin expression using an RNAi approach. Cortical neurons were transfected with Parkin-siRNA or control siRNA at DIV0 and endogenous Parkin levels were then assessed by immunoblot. Parkin-siRNA specifically and efficiently reduced endogenous Parkin expression to 26.10±7.96% (n=3) of control levels (Figure 2E). Knocking down Parkin impaired the elimination of dysfunctional mitochondria, leading to accumulation of mitochondria with reduced TMRE intensity (Figure 2F and 2G). After 24-hr CCCP treatment, 66.91±2.00% of control neurons (n=130) recovered mitochondrial TMRE intensity, versus 19.27±2.01% (n=97, $p<0.001$) of Parkin loss-of-function neurons (Figure 2G). These results support our hypothesis that Parkin-mediated mitophagy is one of the unique neuronal mechanisms to maintain mitochondrial integrity and function in response to dissipating $\Delta\psi_m$. Our RNAi data is consistent with a previous report demonstrating mitochondrial dysfunction and oxidative damage in *Parkin* deficient mice [2].

Previous reports noted an absence of Parkin translocation after acute CCCP treatment of primary cortical neurons [15] and in dopaminergic neurons with the loss of mtDNA [18]. The latter study suggests two different neuronal responses to damaged mitochondria: one for acute $\Delta\psi_m$ dissipation by depolarizing raagents and one for slow progressive deterioration of mitochondrial function by deleting mtDNA *in vivo*. Thus, Parkin-mediated mitophagy likely serves to ensure neuronal mitochondrial integrity by eliminating severely damaged mitochondria with lost $\Delta\psi_m$ [18]. Our study reveals that neuronal mitophagy is a slower process. In response to 24-hr CCCP treatment, only a small percentage of neurons displayed detectable Parkin translocation, while mitochondria in the majority of neurons recover $\Delta\psi_m$. In addition, the efficacy of Parkin-mediated mitophagic flux in neurons is controlled by lysosomal degradation capacity. It is unclear how neurons recover their $\Delta\psi_m$ following prolonged CCCP treatment in culture. Unlike most cells, neurons are wholly dependent upon mitochondrial respiration, thus special mechanisms are required to recover damaged mitochondria after global depolarization. We propose that lysosomal function, proper Parkin expression, slow Parkin translocation, and the elimination of dysfunctional mitochondria are important factors for $\Delta\psi_m$ recovery. In addition, the quality of the neuronal culture is critical to create optimal survival conditions following CCCP treatment; if not met, the uncoupled mitochondria may quickly initiate an apoptotic process before Parkin translocation can be

observed. We have established a high neuronal culture quality to meet our live neuron imaging standards with minimal enzymatic, mechanical, chemical, and oxidative damage [19, 20] (see Supplemental Methods).

Parkin-Targeted Mitochondria Accumulate in the Somatodendritic Regions

We examined the distribution of Parkin-targeted mitochondria in neurons treated with CCCP/LIs. Translocated YFP-Parkin forms typical ring-like structures surrounding fragmented mitochondria, which predominantly accumulate in the soma and proximal dendritic regions, but are hardly detectable in axons and the distal dendritic processes (Figure 3A), suggesting that depolarized mitochondria are selectively accumulated in the somatodendritic regions after prolonged CCCP treatment. Such unique compartmental restriction was consistently observed in neurons treated with a second $\Delta\psi_m$ dissipating reagent antimycin A (1μM) or the selective ATP synthase inhibitor oligomycin (1μM) (Figures S2C–2D, S3).

This unique distribution pattern suggests that depolarized mitochondria undergo altered transport following prolonged CCCP treatment. To test this possibility, we examined relative mitochondrial mobility following 24-hr CCCP treatment. We selected axons for measuring mitochondrial mobility due to their uniform microtubule organization and polarity. Axonal processes were selected as we previously reported [19, 20](Supplemental Methods). Kymographs were used to quantify relative mobility. In DMSO-treated neurons, 42.7±2.3% (mean±SEM) of axonal mitochondria are stationary and 57% of mitochondria are mobile, where 35.9±2% undergo anterograde transport and 21.3±2% undergo retrograde transport. In contrast, in neurons with Parkin translocation, anterograde transport was reduced to 13.3±2% ($p<0.001$) while retrograde transport was relatively increased (36.12±3.67%, $p=0.002$), accompanied by reduced velocity and altered flux of axonal mitochondria (Figure 3B–3D). In recovered neurons without Parkin translocation after CCCP treatment, mobility parameters were similar or slightly changed compared to those in DMSO-treated neurons.

Altered mitochondrial mobility may be protective for neurons under stressful conditions, where healthy mitochondria remain distally while damaged mitochondria return to the soma for degradation. To test this hypothesis, we over-expressed syntaphilin (SNPH), a neuronal mitochondria docking protein that anchors mitochondria to microtubules, to artificially immobilize mitochondria in distal processes [19]. To our surprise, the distribution of Parkin-targeted mitochondria in neurons changed strikingly following CCCP treatment; Parkin was recruited to arrested mitochondria in distal neuronal processes (Figure 3E). This artificial phenotype suggests that once distal mitochondria are immobilized, they will eventually recruit Parkin. Thus, somatodendritic accumulation of Parkin-targeted mitochondria may be coordinately attributed to several factors including (1) reduced anterograde and relatively enhanced retrograde transport leading to more depolarized mitochondria accumulated in the somatodendritic regions during prolonged CCCP treatment and (2) immobilization of mitochondria after slow Parkin translocation, resulting in reduced anterogade flux of damaged mitochondria into distal processes (Figure 3C and 3D). Therefore, a Parkin-mediated process prevents dysfunctional mitochondria from traveling peripherally. Consistently, we observed that Parkin-targeted mitochondria in the soma remain stationary throughout time-lapse recording. This hypothesis is consistent with previous studies showing reduced levels of motor/adaptor proteins upon CCCP-induced mitophagy [12, 13] and a recent report showing that Parkin-dependent degradation of Miro arrests mitochondrial movement [21].

The correlation between $\Delta\psi_m$ and mitochondrial mobility is controversial, especially following acute treatment of neurons with high concentrations of $\Delta\psi_m$ dissipating reagents

[22, 23]. In one study with JC-1 staining and acute depolarization with much higher concentrations of antimycin A (100μM), 90% of mitochondria with high $\Delta\psi_m$ moved in the anterograde direction, whereas 80% with low $\Delta\psi_m$ moved in the retrograde direction [22]. Interestingly, acutely applying a much higher concentration of CCCP (1mM) blocks mitochondrial transport. Another study with TMRM staining showed no correlation between $\Delta\psi_m$ and the direction of axonal mitochondrial transport in sensory neurons [23]. In our study, we instead examined mitochondrial mobility after neuron recovery from 24-hr treatment with a lower concentration of CCCP (10μM), allowing us to assess the correlation between mobility and slow Parkin translocation. Prolonged $\Delta\psi_m$ dissipation may allow the proceeding slow events to induce mobility changes in neurons, which is supported by our observations that only neurons with Parkin translocation displayed reduced anterograde movement.

Parkin-Targeted Mitochondria Are Eliminated through the Autophagy-Lysosomal Pathway in Somas

To determine if Parkin-targeted mitochondria are degraded via the autophagy-lysosomal pathway, we labeled autophagic vacuoles with GFP-LC3 [20]. In DMSO-treated conditions, GFP-LC3 was cytosolic (Figure 4A). However, CCCP treatment resulted in LC3-labeled ring-like structures surrounding fragmented mitochondria in the somatodendritic regions. Treating neurons with both CCCP and LIs produced more LC3-labeled mitochondria (yellow) and other autophagic vacuoles (green). These imaging results are consistent with our biochemical observations showing elevated LC3-II and p62 levels in the mitochondria-enriched fraction following depolarization (Figure 1F). To determine whether depolarized mitochondria were retained within lysosomal organelles upon lysosomal inhibition, we expressed GFP-LAMP1, a lysosomal membrane protein. In DMSO-treated neurons, there was little co-localization (2.72±0.31%) between mitochondria and lysosomes (Figures 4B). In contrast, treatment with CCCP/LIs significantly enhanced the recruitment of mitochondria to LAMP1-labeled lysosomes in the soma (32.10±2.17%, $p<0.001$). This indicates that proper lysosomal function is required to efficiently eliminate damaged mitochondria.

We next examined Parkin and LC3-labled mitochondrial dynamics in the somatodendritic regions (Figure 4C). During a 25-min time-lapse recording of the soma, ring-like vesicular structures co-labeled with GFP-LC3 and mCherry-Parkin disappeared whereas new puncta emerged. Furthermore, a ring-like Parkin-associated mitochondrion, as opposed to the Parkin-negative mitochondria in the same image, disappeared over a 38-min time-lapse recording period (Figure 4D, Movie 2). Both the Parkin-ring structure and the mitochondrion were eliminated while the Parkin-unlabeled mitochondrion remained. Thus, our study provides live neuronal evidence showing degradation of Parkin-targeted mitochondria through the autophagy-lysosomal pathway.

Although somatodendritic Parkin-mediated mitophagy is readily and consistently detected in our cultures, it was hardly detectable along distal axonal processes. Alternatively, GFP-LC3 in cortical neurons was recruited to axonal mitochondria following 24-hr treatment with CCCP/LIs (Figure S4). Thus, axonal mitochondria may undergo either Parkin-mediated mitophagy at undetectable Parkin signals or Parkin-independent mitophagy. Further investigation is required to determine the main mechanism for axonal mitochondrial quality control.

Dysfunctional mitochondria not only produce energy less efficiently, but also release harmful reactive oxygen species and initiate apoptotic signaling cascades, all linked to the pathogenesis of major neurodegenerative disorders [24–28]. Sequestration and elimination of aged and damaged mitochondria is an important but poorly characterized neuronal

mechanism. In the current study, we reveal several unique features of Parkin-mediated mitophagy in mature cortical neurons. First, Parkin translocation onto mitochondria is slower than in non-neuronal cells. Second, Parkin is selectively recruited to depolarized mitochondria to form ring-like structures. Third, following 24-hr CCCP incubation, Parkin translocation only occurs in a small percentage of neurons. Lysosomal degradation is critical for the efficacy of Parkin-mediated mitophagy. Fourth, Parkin translocation is restricted to the somatodendritic regions, where mature and acidic lysosomes are predominantly localized [20, 29–30]. This spatial and dynamic process allows neurons to efficiently eliminate dysfunctional mitochondria. Therefore, our study, for the first time, shows selective and dynamic Parkin translocation to depolarized mitochondria and subsequent degradation via the autophagy-lysosomal pathway in live neurons.

Four Bullets

Depolarized mitochondria recruit exogenous/endogenous Parkin in mature cortical neurons

Parkin translocation occurs predominantly in the somatodendritic region

Dynamic elimination of Parkin and LC3-targted depolarized mitochondria in the soma

Knocking down Parkin in neurons impairs the elimination of dysfunctional mitochondria

Supplementary Material

Refer to Web version on PubMed Central for supplementary material.

Abbreviation

$\Delta\psi_m$	mitochondrial membrane potential
CCCP	Carbonyl Cyanide m-Chlorophenylhydrazone
DIV	days *in vitro*
LAMP1	lysosome-associated membrane protein-1
LC3	microtubule-associated protein light chain 3
LIs	lysosomal inhibitors
Mito	mitochondria
MT	microtubule
TMRE	Tetramethylrhodamine ethyl ester
Parkin	a cytosolic E3 ubiquitin ligase

Acknowledgments

We thank R.J. Youle for helpful discussions; R.J. Youle, B. Lu, and M.J. LaVoie for Parkin DNA constructs; the members of the Sheng lab for technical assistance and helpful discussions; S. Yang and D. Schoenberg for editing. This work was supported by the Intramural Research Program of NINDS, NIH (Z-H. S.), the NIH Pathway to Independence Award K99 (Q. C.), and HHMI-NIH Research Scholars Program (H.M. Z.)

References

1. Greene JC, Whitworth AJ, Kuo I, Andrews LA, Feany MB, Pallanck LJ. Mitochondrial pathology and apoptotic muscle degeneration in Drosophila parkin mutants. Proc. Natl. Acad. Sci. USA. 2003; 100:4078–4083. [PubMed: 12642658]
2. Palacino JJ, Sagi D, Goldberg MS, Krauss S, Motz C, Wacker M, Klose J, Shen J. Mitochondrial dysfunction and oxidative damage in parkin-deficient mice. J. Biol. Chem. 2004; 279:18614–18622. [PubMed: 14985362]
3. Clark IE, Dodson MW, Jiang C, Cao JH, Huh JR, Seol JH, Yoo SJ, Hay BA, Guo M. Drosophila pink1 is required for mitochondrial function and interacts genetically with parkin. Nature. 2006; 441:1162–1166. [PubMed: 16672981]
4. Gautier CA, Kitada T, Shen J. Loss of PINK1 causes mitochondrial functional defects and increased sensitivity to oxidative stress. Proc. Natl. Acad. Sci. USA. 2008; 105:11364–11369. [PubMed: 18687901]
5. Deng H, Dodson MW, Huang H, Guo M. The Parkinson's disease genes pink1 and parkin promote mitochondrial fission and/or inhibit fusion in Drosophila. Proc. Natl. Acad. Sci. USA. 2008; 105:14503–14508. [PubMed: 18799731]
6. Yang Y, Ouyang Y, Yang L, Beal MF, McQuibban A, Vogel H, Lu B. Pink1 regulates mitochondrial dynamics through interaction with the fission/fusion machinery. Proc. Natl. Acad. Sci. USA. 2008; 105:7070–7075. [PubMed: 18443288]
7. Poole AC, Thomas RE, Andrews LA, McBride HM, Whitworth AJ, Pallanck LJ. The PINK1/Parkin pathway regulates mitochondrial morphology. Proc. Natl. Acad. Sci. USA. 2008; 105:1638–1643. [PubMed: 18230723]
8. Yu W, Sun Y, Guo S, Lu B. The PINK1/Parkin pathway regulates mitochondrial dynamics and function in mammalian hippocampal and dopaminergic neurons. Hum. Mol. Genet. 2011; 20:3227–3240. [PubMed: 21613270]
9. Narendra D, Tanaka A, Suen DF, Youle RJ. Parkin is recruited selectively to impaired mitochondria and promotes their autophagy. J. Cell Biol. 2008; 183:795–803. [PubMed: 19029340]
10. Geisler S, Holmstrom KM, Skujat D, Fiesel FC, Rothfuss OC, Kahle PJ, Springer W. PINK1/Parkin-mediated mitophagy is dependent on VDAC1 and p62/SQSTM1. Nat. Cell Biol. 2010; 12:119–131. [PubMed: 20098416]
11. Matsuda N, Sato S, Shiba K, Okatsu K, Saisho K, Gautier CA, Sou YS, Saiki S, Kawajiri S, Sato F, et al. PINK1 stabilized by mitochondrial depolarization recruits Parkin to damaged mitochondria and activates latent Parkin for mitophagy. J. Cell Biol. 2010; 189:211–221. [PubMed: 20404107]
12. Chan NC, Salazar AM, Pham AH, Sweredoski MJ, Kolawa NJ, Graham RL, Hess S, Chan DC. Broad activation of the ubiquitin-proteasome system by Parkin is critical for mitophagy. Hum. Mol. Genet. 2011; 20:1726–1737. [PubMed: 21296869]
13. Yoshii SR, Kishi C, Ishihara N, Mizushima N. Parkin mediates proteasome-dependent protein degradation and rupture of the outer mitochondrial membrane. J. Biol. Chem. 2011; 286:19630–19640. [PubMed: 21454557]
14. Seibler P, Graziotto J, Jeong H, Simunovic F, Klein C, Krainc D. Mitochondrial Parkin recruitment is impaired in neurons derived from mutant PINK1 induced pluripotent stem cells. J. Neurosci. 2011; 31:5970–5976. [PubMed: 21508222]
15. Van Laar VS, Arnold B, Cassady SJ, Chu CT, Burton EA, Berman SB. Bioenergetics of neurons inhibit the translocation response of Parkin following rapid mitochondrial depolarization. Hum. Mol. Genet. 2011; 20:927–940. [PubMed: 21147754]
16. Van Humbeeck C, Cornelissen T, Hofkens H, Mandemakers W, Gevaert K, De Strooper B, Vandenberghe W. Parkin interacts with Ambra1 to induce mitophagy. J. Neurosci. 2011; 31:10249–10261. [PubMed: 21753002]
17. Vives-Bauza C, Zhou C, Huang Y, Cui M, de Vries RL, Kim J, May J, Tocilescu MA, Liu W, Ko HS. PINK1-dependent recruitment of Parkin to mitochondria in mitophagy. Proc. Natl. Acad. Sci. USA. 2010; 107:378–383. [PubMed: 19966284]

18. Sterky FH, Lee S, Wibom R, Olson L, Larsson NG. Impaired mitochondrial transport and Parkin-independent degeneration of respiratory chain-deficient dopamine neurons in vivo. Proc. Natl. Acad. Sci. USA. 2011; 108:12937–12942. [PubMed: 21768369]

19. Kang JS, Tian JH, Pan PY, Zald P, Li C, Deng C, Sheng ZH. Docking of axonal mitochondria by syntaphilin controls their mobility and affects short-term facilitation. Cell. 2008; 132:137–148. [PubMed: 18191227]

20. Cai Q, Lu L, Tian JH, Zhu YB, Qiao H, Sheng ZH. Snapin-regulated late endosomal transport is critical for efficient autophagy-lysosomal function in neurons. Neuron. 2010; 68:73–86. [PubMed: 20920792]

21. Wang X, Winter D, Ashrafi G, Schlehe J, Wong YL, Selkoe D, Rice S, Steen J, LaVoie MJ, Schwarz TL. PINK1 and Parkin target Miro for phosphorylation and degradation to arrest mitochondrial motility. Cell. 2011; 147:893–906. [PubMed: 22078885]

22. Miller KE, Sheetz MP. Axonal mitochondrial transport and potential are correlated. J. Cell Sci. 2004; 117:2791–2804. [PubMed: 15150321]

23. Verburg J, Hollenbeck PJ. Mitochondrial membrane potential in axons increases with local nerve growth factor or semaphorin signaling. J Neurosci. 2008; 28:8306–8315. [PubMed: 18701693]

24. Chen H, Chan DC. Mitochondrial dynamics--fusion, fission, movement, and mitophagy--in neurodegenerative diseases. Hum. Mol. Genet. 2009; 18:R169–R176. [PubMed: 19808793]

25. Lin MT, Beal MF. Mitochondrial dysfunction and oxidative stress in neurodegenerative diseases. Nature. 2006; 443:787–795. [PubMed: 17051205]

26. Schon EA, Przedborski S. Mitochondria: the next (neurode)generation. Neuron. 2011; 70:1033–1053. [PubMed: 21689593]

27. Schapira AH. Mitochondria in the aetiology and pathogenesis of Parkinson's disease. Lancet Neurol. 2008; 7:97–109. [PubMed: 18093566]

28. Sheng ZH, Cai Q. Mitochondrial transport in neurons: impact on synaptic homeostasis and neurodegeneration. Nat. Rev. Neurosci. 2012 Jan 5. Epub ahead of print.

29. Overly CC, Hollenbeck PJ. Dynamic organization of endocytic pathways in axons of cultured sympathetic neurons. J. Neurosci. 1996; 16:6056–6064. [PubMed: 8815888]

30. Lee S, Sato Y, Nixon RA. Lysosomal proteolysis inhibition selectively disrupts axonal transport of degradative organelles and causes an Alzheimer's-like axonal dystrophy. J Neurosci. 2011; 31:7817–7830. [PubMed: 21613495]

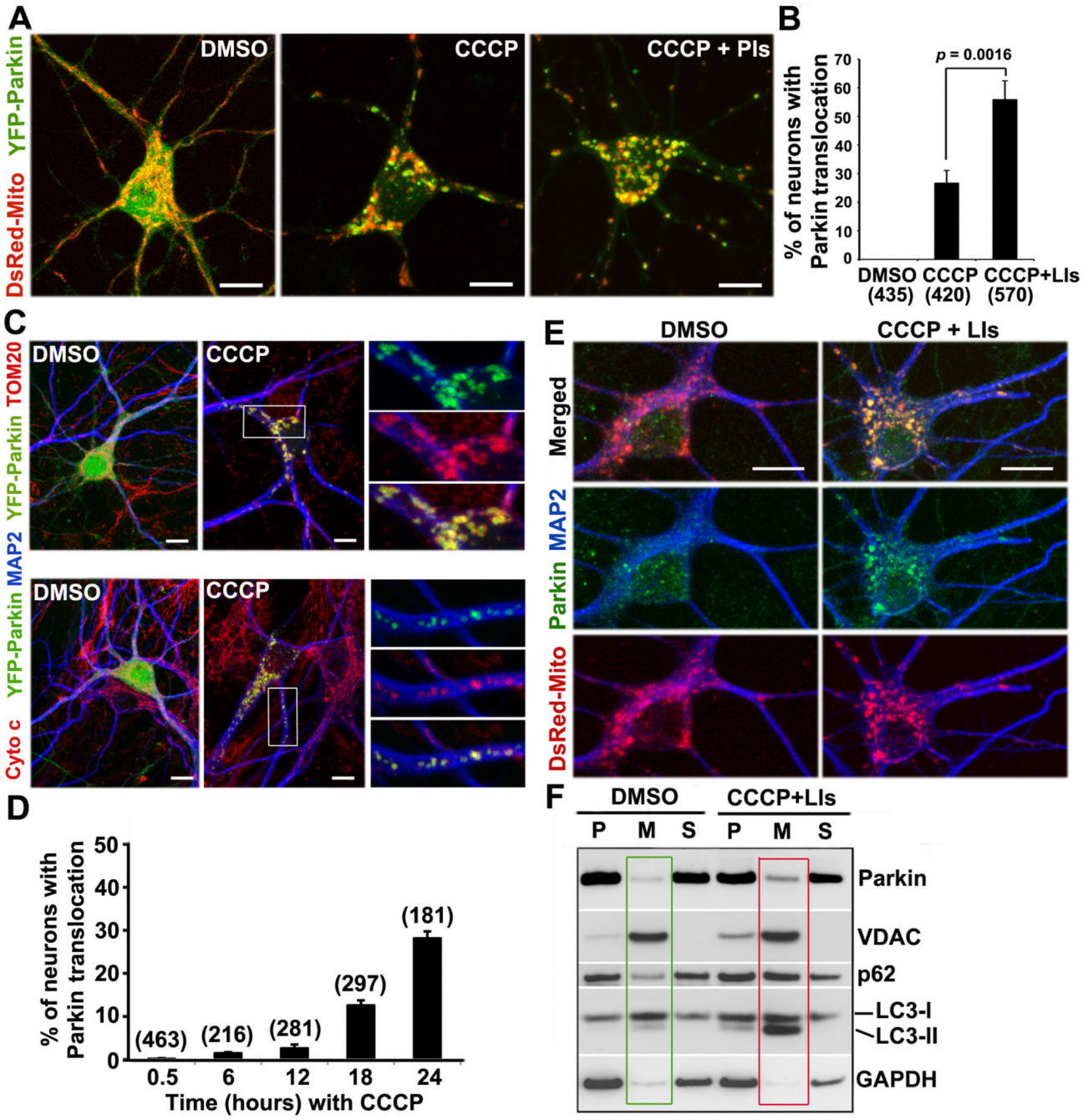

Figure 1. CCCP-Induced Recruitment of Parkin to Mitochondria in Cortical Neurons

(A, B) Representative images (A) and quantitative analysis (B) showing CCCP-induced Parkin translocation to mitochondria. Cortical neurons expressing YFP-Parkin and DsRed-Mito at DIV9 were treated for 24 hr with DMSO, 10μM CCCP, or 10μM CCCP + lysosomal inhibitors (LIs).

(C) CCCP-induced Parkin translocation to mitochondria labeled by mitochondrial marker TOM20 (upper panels) or cytochrome *c* (lower panels). Cortical neurons expressing YFP-Parkin were treated with DMSO or 10μM CCCP followed by co-immunostaining with antibodies against MAP2 and TOM20 or cytochrome *c*. The right three panels show enlarged views of the boxed area.

(D) Time course of Parkin translocation following depolarization. Neurons at DIV8-10 were imaged at sequential time points during CCCP treatment.
(E) Endogenous Parkin translocation to mitochondria. Cortical neurons expressing DsRed-Mito at DIV10 were treated with DMSO or CCCP/LIs for 24 hr, followed by immunostaining with a monoclonal Parkin antibody (Abcam). Note that CCCP/LIs treatment induces the recruitment of endogenous Parkin to mitochondria.
(F) Increased endogenous Parkin associates with mitochondria following CCCP/LIs treatment (red box) relative to that with DMSO control (green box). Cortical neurons at DIV13 were incubated with DMSO or 10μM CCCP/LIs for 24 hr and then subjected to fractionation into post-nuclear supernatant (P), mitochondria-enriched membrane pellet (M), and cytosol supernatant (S). 10μg of protein was sequentially immunoblotted with antibodies against Parkin (monoclonal, Santa Crutz) and various markers including VDAC (mitochondria), GAPDH (cytosol), p62/SQSTM1 and LC3 (autophagy).
Scale bars: 10μm. Data was quantified from the number of neurons indicated in parentheses from 3–4 independent experiments. Error bars: SEM. Student's *t* test.

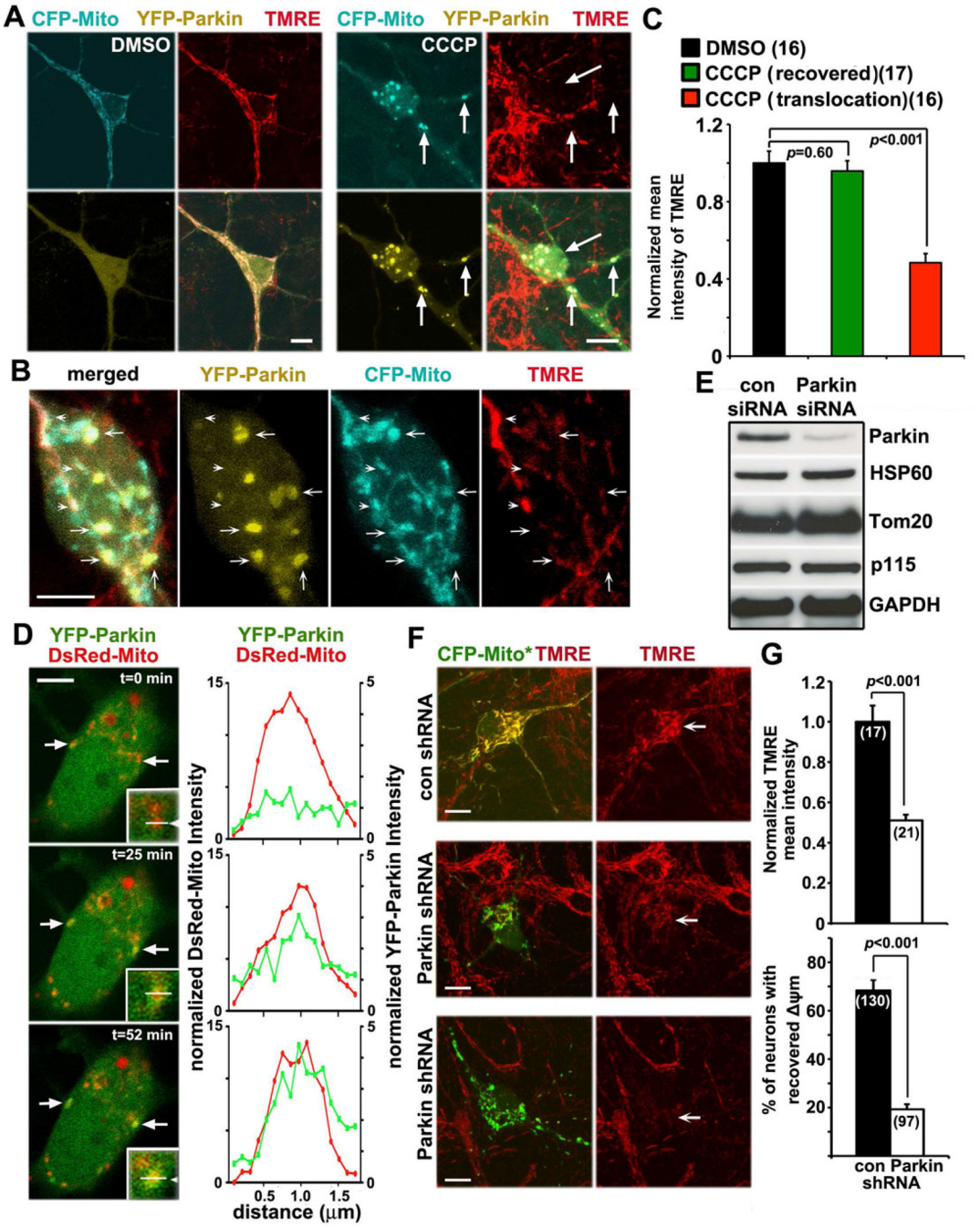

Figure 2. Selective Parkin Recruitment to Depolarized Mitochondria

(A–C) Representative images (A, B) and quantitative analysis (C) showing translocation of YFP-Parkin to depolarized mitochondria. Cortical neurons expressing YFP-Parkin and CFP-Mito at DIV9 were treated with DMSO or 10μM CCCP for 24 hr followed by loading with mitochondrial $\Delta\psi_m$-dependent dye TMRE for 30 min prior to imaging. Arrows indicate depolarized mitochondria labeled by CFP-Mito but unlabeled by TMRE. Arrowheads represent polarized mitochondria marked by both CFP-Mito and TMRE, which are un-labeled by Parkin. TMRE mean intensity was normalized to DMSO control neurons. Note that neurons recovered from CCCP-treatment maintain normal TMRE mean intensity

($p<0.60$) while neurons displaying Parkin translocation have reduced TMRE mean intensity in the soma ($p<0.001$) relative to that of control neurons.

(D) Time-lapse imaging of live cortical neurons showing slow and dynamic recruitment of YFP-Parkin to mitochondria in the soma. Neurons were treated for 24 hr with 10μM CCCP, followed by 52 min time-lapse imaging. Graphs to the right are line scans of relative DsRed-mito and YFP-Parkin fluorescence intensities in the images at respective time points (left panels).

(E) siRNA-mediated Parkin knock down in neurons. Cortical neurons were transfected with Parkin-siRNA or control siRNA at DIV0 and protein was harvested at DIV4. 10μg of total protein was sequentially immunoblotted with antibodies against Parkin and various markers including HSP60 and Tom20 (mitochondria), p115 (Golgi), GAPDH (cytosol).

(F, G) Representative images (F) and quantitative analysis (G) showing accumulation of depolarized mitochondria by knocking down Parkin in cortical neurons, leading to more mitochondria with reduced or no TMRE staining following CCCP treatment. Arrows point to mitochondria with high TMRE intensity (con-shRNA) or low TMRE intensity (Parkin-shRNA). CFP-Mito*: color converted from cyan to green for better contrast. Quantitative data was expressed as normalized TMRE mean intensity in the soma (upper graph) or % of neurons with recovered TMRE intensity following CCCP treatment (lower graph).

Data was collected from the number of neurons indicated in parentheses from 3 independent experiments. Scale bars in A and F: 10μm; in B and D: 5μm. Error bars: SEM. Student's *t* test.

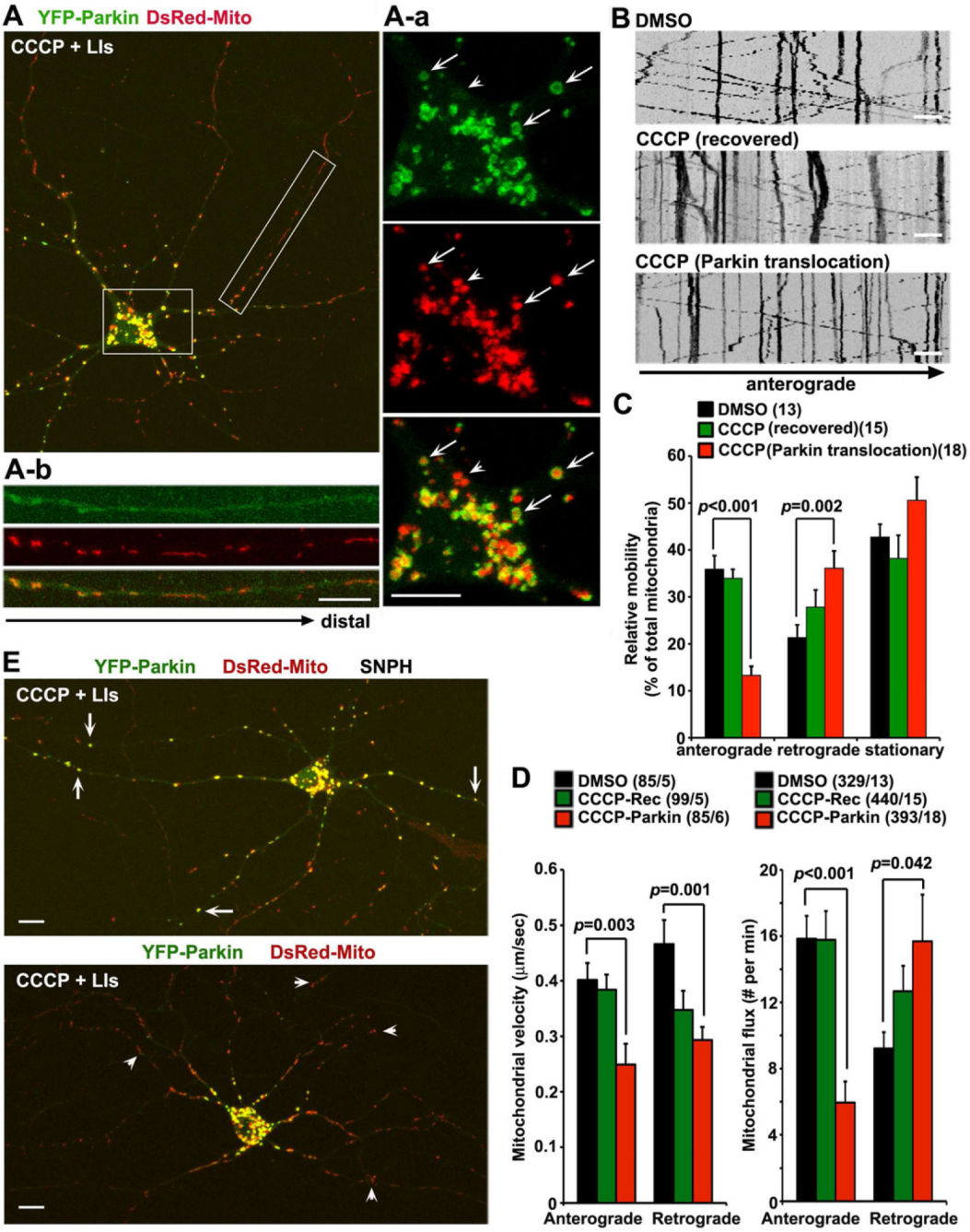

Figure 3. Altered Mitochondrial Transport During Slow Parkin translocation

(A) Representative images showing CCCP-induced Parkin translocation to mitochondria accumulated in the somatodendritic regions. Cortical neurons at DIV9 were treated for 24 hr with 10μM CCCP/LIs. Panels (A–a) show enlarged views of the boxed somatodendritic area. Arrows indicate Parkin ring-like structures surrounding fragmented mitochondria while an arrowhead marks mitochondria unlabeled by Parkin. Panels (A–b) are enlarged views of a dendritic process showing no Parkin-labeled mitochondria at distal regions. (B–D) Representative kymographs (B) and quantitative analysis (C, D) showing that Parkin translocation is accompanied by altered mobility, velocity, and flux of axonal mitochondria. Cortical neurons at DIV9 were treated with DMSO or 10μM CCCP for 24 hr, followed by

15-min time-lapse recordings. Vertical lines represent stationary organelles; oblique lines or curves to the right represent anterograde transport; and lines to the left indicate retrograde movement. Relative mitochondrial mobility was quantified from the number of neurons (C) or the number of mitochondria and axons (D) indicated in parentheses. Note that neurons recovered from CCCP display normal or slightly altered transport while neurons with Parkin translocation show significant changes in mitochondrial mobility.

(E) Immobilizing mitochondria by expressing syntaphilin (SNPH) results in Parkin recruitment to distal mitochondria. Cortical neurons co-expressing SNPH (upper panel) or without SNPH over-expression (lower panel) were treated with CCCP/LIs for 24 hr at DIV9. Arrows point to Parkin-targeted distal mitochondria and arrowheads indicate Parkin-negative distal mitochondria in a control neuron.

Error bars: SEM. Student's *t* test. Scale bars: 10μm.

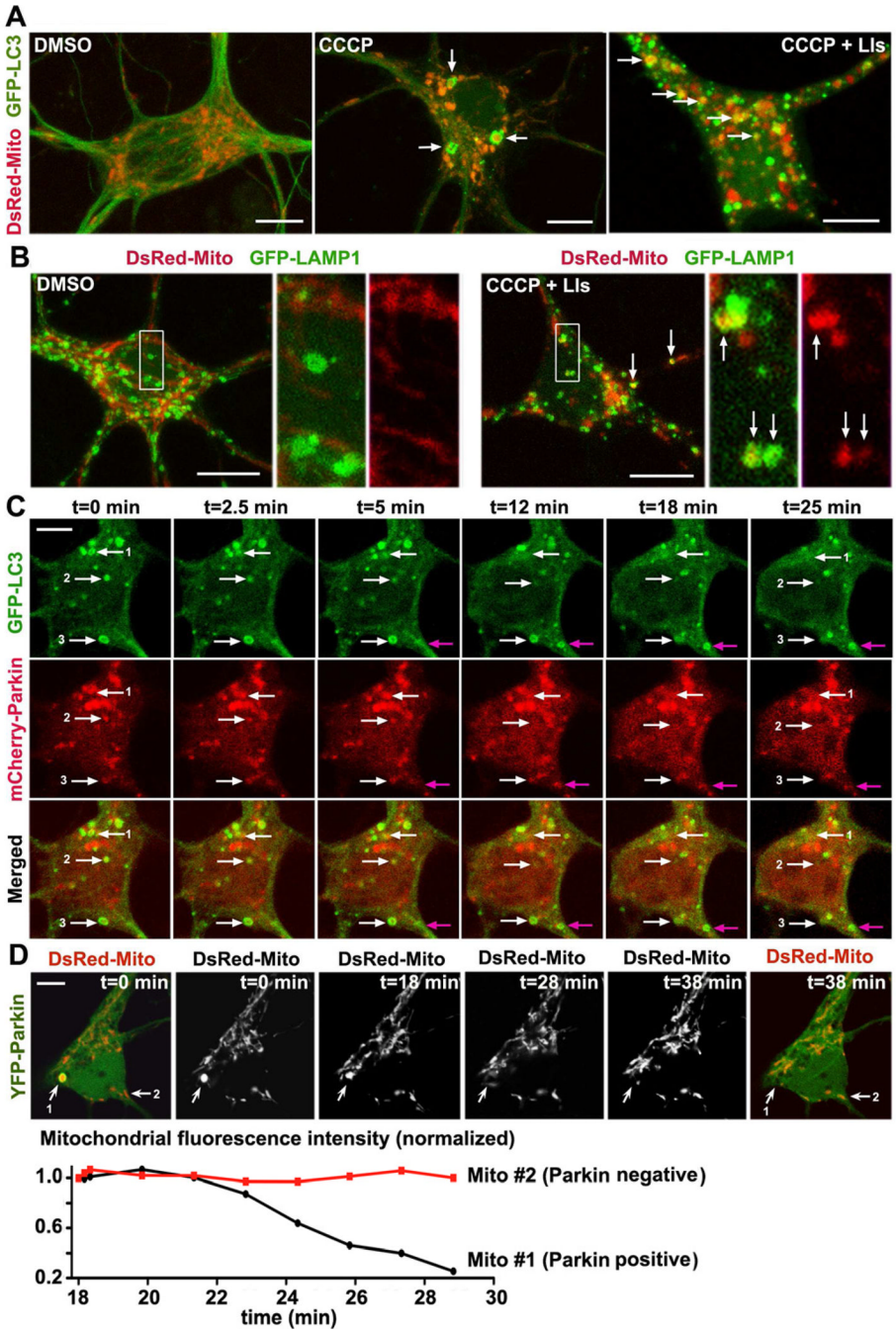

Figure 4. Parkin-Targeted Mitochondria Are Degraded through the Autophagy-Lysosomal Pathway in the Somatodendritic Regions

(A) Representative images showing CCCP-induced LC3 recruitment to depolarized mitochondria. Cortical neurons expressing GFP-LC3 and DsRed-Mito at DIV9 were treated with DMSO, 10μM CCCP, or 10μM CCCP/LIs for 24 hr. Arrows indicate co-localization of mitochondria with GFP-LC3.

(B) CCCP-induced co-localization of mitochondria and lysosomes (indicated by arrows). Neurons expressing GFP-LAMP1 and DsRed-Mito at DIV9 were treated with DMSO or 10μM CCCP/LIs for 24 hr.

(C) Time-lapse imaging showing dynamic emergence and disappearance of Parkin and LC3-labeled autophagic vacuoles in the somatodendritic regions. Neurons expressing GFP-LC3 and mCherry-Parkin were treated for 24 hr with 10μM CCCP, followed by time-lapse imaging. While co-localized ring-like structures of mCherry-Parkin and GFP-LC3 (white arrows) gradually disappeared, some new puncta (red arrows) emerged during the 25-min recording time.

(D) Time-lapse imaging showing disappearance of a Parkin-associated mitochondrion (#1) in the soma following treatment with 10μM CCCP. Lower panel shows normalized DsRed-Mito fluorescence intensity of the mitochondrion #1 (Parkin-positive) and #2 (Parkin-negative). Fluorescence intensity for Mito #1 gradually disappears during a 38-min recording period. DsRed-mito fluorescence intensity of Mito #2 remained consistent throughout the imaging acquisition. Fluorescence intensity of each mitochondrion was normalized to their intensity at t=18 min. Scale bars in A and B: 10μm; in C and D: 5μm.